Electronic structure of $Pb_{1-x}Sr_xS$. Application of the Haydock recursion method

L. C. Davis
Research Staff, Ford Motor Company, Dearborn, Michigan 48121-2053
(Received 27 July 1983)

The Haydock recursion method is used to study the electronic structure of the pseudobinary alloy semiconductor $Pb_{1-x}Sr_xS$. Density of states and $\vec{k}$-dependent spectral weight functions are calculated for a tight-binding model. Large deviations from virtual-crystal behavior are found. The density of cation s states decreases below the valence band and increases above the gap as x increases from 0 to 1. For Pb-rich alloys, the absorption edge (due to the direct gap at L) goes from the infrared to the visible as Sr is added, in agreement with experiment. Near $x=1$ (Sr rich), the direct gap at X increases slightly as the Pb concentration is increased. The gap in the density of states and the optical-absorption edge decreases, however, due to the formation on an electron-volt scale of an impurity band comprised mostly of Pb p states. The advantages of the recursion method relative to the coherent-potential approximation for calculating the electronic structure of alloys are discussed. It is concluded that the recursion method represents a viable alternative for real materials.

I. INTRODUCTION

Holloway and Jesion[1] have reported a new pseudobinary alloy $Pb_{1-x}Sr_xS$ which exists as a single phase over the entire composition range $0<x<1$. The optical absorption edge varies continuously and monotonically from 0.4 eV for PbS to 4.6 eV for SrS. The ability to tailor the edge to any value between these limits by adjusting the composition is clearly significant. In the present work, understanding the electronic structure of this alloy is the primary consideration.

The electronic structure of $Pb_{1-x}Sr_xS$ is interesting because the cations Pb and Sr differ so much that an average cation potential is meaningless. Pb is a group-IV element whereas Sr is a group-II element. Roughly speaking, the Pb ion has the configuration $6s^2$ in PbS; its two $6p$ electrons are donated to the S anion to complete the sulfur $3p$ subshell (configuration $3p^6$). The $6s$ electrons form a narrow band well below the forbidden energy gap[2] (see Fig. 1). The S $3p$ and the Pb $6p$ form bonding and antibonding bands—the valence and conduction bands. Sr, on the other hand, has an atomic configuration of $5s^2$ and in SrS donates these two electrons to the S ion. In SrS the valence band is predominantly S $3p$ and the conduction band consists of Sr $5s$ plus other orbitals.[3] The cation s character goes from below the valence band in PbS to the conduction band in SrS, but does not pass through the gap. One cannot continuously distort the PbS bands to form the SrS bands and simultaneously describe the alloys of intermediate concentrations. That is, the virtual-crystal approximation[4] fails. It will be shown that a physically more correct picture is that the s density of states (DOS) decreases below the gap and increases above as x increases.

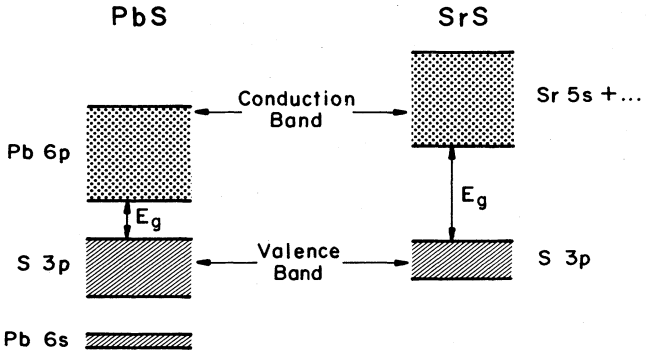

FIG. 1. Schematic drawing of the bands in PbS and SrS. Each band is labeled by the dominant atomic constituent. The cation s states go from below the valence band in PbS to being part of the conduction band in SrS. The energy gap E_g is indicated for each material.

To handle this problem, a rather new technique, which has been used for related problems,[5,6] is adopted for the present work. This technique is based upon the Haydock recursion method[7] which gives a numerically convenient way of calculating partial (or projected) DOS. Although large, but finite clusters of atoms are used in the computations, results are inferred for infinite systems. The technique essentially sacrifices precision or resolution (more so than accuracy) for increased speed and reduced amount of computation.

The recursion method as applied in the present work has several advantages over the coherent-potential approximation (CPA), the method commonly used for semiconductor alloy calculations.[4,8–10] The most fundamental is that no effective-medium theory is imposed, i.e., the effects of the detailed local configurations are not omitted. The approach used here is physically more transparent than the CPA and fits in well with impurity calculations. It is easy to use since the Cambridge Recursion Library

routines are readily available,[11] and is in many instances easier to use than the CPA. Finally, it is attractive since the results can be made as close to the exact results as desired by expending more computational effort (i.e., larger clusters and more recursions). In contrast, systematic improvement of the CPA is difficult. Currently there are, however, some limitations with the recursion method which will become apparent in subsequent sections (also see Ref. 5).

The plan of the paper is as follows. The band structures of PbS and SrS are discussed in Sec. II, and a model for the alloy is determined. The recursion method and the formal theory are given in Sec. III. Numerical results and their interpretation are presented in Sec. IV. The conclusions are summarized in Sec. V.

II. BAND STRUCTURE AND TIGHT-BINDING MODEL

In this section a tight-binding model is developed to describe the band structure of PbS and SrS. The parameters of the model are the usual atomic energies and near-neighbor matrix elements. These parameters will be used in conjunction with the recursion method described in the next section to calculate the electronic structure of the alloys. The band structure of PbS is well known; the most accurate calculation is probably the pseudopotential results of Kohn *et al.*[12] Unfortunately, the insulator SrS is more difficult to treat properly and the only reported results do not agree with the fundamental gap very well.[3] Hence our determination of the SrS parameters will be somewhat tentative until a better band structure is available.

The choice of using a tight-binding model rather than pseudopotentials was made primarily because the recursion method (in its usual form) requires it. Also, a tight-binding model is simple, whereas a more nearly *a priori* method [orthogonalized plane wave (OPW), augmented plane wave (APW), or CPA with muffin-tin potential for the alloy[13,14]] is beyond the scope of the present work. As is common, a good description of the valence bands and the tightly bound states can be obtained. The conduction band cannot be described as well, but a reasonable approximation to the conduction-band edge has been found. Higher-lying bands will not be physically meaningful to any great extent, but will be used principally to perturb (shift) lower-energy bands of the same symmetry, in the manner of peripheral states.[15,16]

It has been found that a basis set consisting of s, p, and d functions on both cation and anion is adequate for our purposes. The set is assumed to be orthonormal with no overlap matrix elements between functions on different sites. (For justification of this assumption, see the discussion given by Bullet in Ref. 7, p. 129.) To save a factor of 2 in size, spin-orbit interactions are neglected. Although relativistic effects are important in PbS (and are parametrically included in our model), the splittings caused by spin-orbit interaction are not crucial here. For simplicity, a nonrelativistic notation for the bands will be used.

The crystal structure is rocksalt, and the lattice constant changes by about 1% from PbS to SrS. It is assumed that the Pb-S and Sr-S interactions do not change across the alloy composition range. Also, the assumption is made that the atomic energies remain constant.

The parameters of the tight-binding model are defined and their values given in Tables I–III and Fig. 2. In the Appendix, the band energies at symmetry points are given in terms of these parameters. These expressions were used in the fitting procedure to determine the parameters.

Let us first consider PbS (see Fig. 3). The principal bonding is between the Pb p orbitals and the S p orbitals. A Pb p_x function at the origin, for example, strongly interacts with a S p_x at $(a/2,0,0)$, forming a σ bond. The matrix element is denoted by V_{xx} and is the dominant interaction determining the mixing of Pb and S levels. The only other independent p-p interaction between nearest neighbors is the weaker π-bonding matrix element V_{zz}. Even if we were to neglect all other interactions, there would still be a large splitting (~ 7 eV) at Γ ($\vec{k}=\vec{0}$) and at X $[(2\pi/a)(1,0,0)]$, the off-diagonal matrix element being $2(V_{xx}-2V_{zz})$ for Γ_{15} and $2V_{xx}$ for $X_{5'}$. At L $[(2\pi/a)(\frac{1}{2},\frac{1}{2},\frac{1}{2})]$, symmetry forbids an interaction due to p-p interactions and in lowest order the anion p states (L_1 and L_3) should have energy $E_p^{(A)}$ and the cation states ($L_{2'}$ and $L_{3'}$) $E_p^{(C)}$. $E_p^{(A)}$ and $E_p^{(C)}$ are the atomic energies for p states on the anions and cations, respectively.

The next order of interaction, due to the matrix element V_{sp} between Pb s and S p, shifts the energies at L. (Note that where order is important, the first subscript indicates the cation orbital and the second the anion). In a previous publication[17] this interaction and its influence on Pb impurity levels in SrS were discussed. Here it is sufficient to note that the L_1 level due to Pb s electrons at -7.9 eV is mixed with the S p L_1 level, which is the top of the valence band. The matrix element is $2(3)^{1/2}V_{sp}$ and produces a shift of ~ 2 eV (upward for the valence-band edge and downward for the Pbs–derived state). Symmetry does not allow s-p mixing at Γ or X. Some cation–d-anion p interaction is included, e.g., a shift of 0.5 eV downward in the L_1 (valence-band edge) energy is due to a matrix element between Pb d (t_{2g}) and S 3p.

To complete the discussion of the interactions affecting the valence band, it should be remarked that a sulfur-sulfur interaction of the type described by Pantelides[18] is also included. The two pertinent matrix elements, a p bonding V_p (like a σ bond) and a π bonding V_π, are determined from the SrS valence bands[17] where the bandwidth is due mostly to this interaction. (The matrix elements are assumed constant across the composition range.)

The conduction-band edge in PbS is at $L_{2'}$, and it is made up of Pb p states in addition to anion s and d (t_{2g}) states. The s state can be thought of as the S 4s atomic state, although it is more correct to regard it as a peri-

TABLE I. Atomic energies (eV).

Orbital	Pb	Sr	S
s	-5.7	7.1	15.0
p	3.63	15.0	-0.73
$d(e_g)$	6.0	7.0	15.0
$d(t_{2g})$	10.0	8.2	15.0

TABLE II. Nearest-neighbor matrix elements (eV). Notation: V_{sp} means cation s, anion p, V_{ps} means cation p, anion s, etc.; refer to Fig. 2.

(0,0,0)	$(a/2,0,0)$	Symbol	PbS	SrS
s	s	V_{ss}	0.0	−0.403
s	p_x	V_{sp}	1.047	0.65
		V_{ps}	1.783	2.341
p_x	p_x	V_{xx}	2.499	1.5
p_z	p_z	$-V_{zz}$	−0.219	0.0
p_x	x^2-y^2	$-3^{1/2}V_{pd}$	see below	
		$-3^{1/2}V_{dp}$	see below	
p_x	$3z^2-r^2$	V_{pd}	0.922	0.0
		V_{dp}	0.970	0.536
xy	p_y	V_{xyp}	0.617	0.25
		V_{pxy}	0.75	0.0
xy	xy	V_{xyxy}	1.645	1.611
yz	yz	$-V_{yzyz}$	−0.563	−0.486

pheral state used to push $L_{2'}$ down. That is, it is a representation of higher-lying bands of the same symmetry which perturb the state. The tight-binding approximation is not as applicable to the conduction band as to the valence band, so we cannot interpret the states too literally. Inclusion of a Pb-Pb interaction in the model did not improve the fit to the band structure appreciably.

The d states, in particular the t_{2g}, could have been neglected without serious effect on the fit for PbS if only the region around the gap and below were of interest. However, they were introduced so that the X_3 conduction-band state at 4.4 eV would exist in the model. This state is of t_{2g} symmetry and has no p or s components. The X_3 state is thought to be the conduction-band edge in SrS,[3] and it is desirable to follow its behavior across the alloy composition range. The gap in PbS is direct and is at L.

With this many parameters a rather good fit to the valence bands and lowest conduction bands was obtained, although the set of parameters given in Tables I—III is not necessarily optimal. The model band structure is shown in Fig. 3 and compares favorably with Fig. 9 of Kohn *et al.*[12]

The band structure of SrS is much less certain than that of PbS. Limited experimental information is available, primarily optical absorption data. Hasegawa and Yanase[3] have done a nonrelativistic, self-consistent APW calculation with Slater exchange. They found a direct band gap at X ($X_{5'}$ to X_3) with energy of 3.11 eV and a smaller, indirect gap (Γ_{15} to X_3) of 2.66 eV. An indirect gap with small absorption cannot be ruled out on the basis of available experimental information. Since SrS is an insulator, it may not be too surprising that correlation effects which are difficult to treat properly may affect the gap energy.

TABLE III. Next-nearest-neighbor matrix elements (eV); refer to Fig. 2.

Matrix element	Pb-Pb	Sr-Sr	S-S	Pb-Sr
V_s(s—s bonding)	0.0	−0.13	0.0	0.0
V_p(σ bonding)	0.0	0.0	0.21	0.0
V_π(π bonding)	0.0	0.0	0.0325	0.0

To correct the disagreement with experiment, the approach used here was to move up the conduction bands of Hasegawa and Yanase, adjusting the X_3-$X_{5'}$ separation to the measured gap (4.6 eV). (See Fig. 4; the direct gap may be somewhat larger than this value since the absorption edge probably corresponds to an exciton.[19]) The bands were then fitted approximately with the tight-binding model. The Sr p levels play only a minor role, being relegated to the status of high-energy peripheral states. The conduction band is comprised mostly of Sr s and d states. A Sr-Sr interaction between s electrons, V_s, is included to give dispersion to the conduction band originating from Γ_1. The dispersion of the band connecting to X_3 is attributed to t_{2g}-t_{2g} interactions. Not all of the d-d interactions are included, so the high-lying d states in the model (mostly occurring above the region of interest) are probably too flat.

The valence-band dispersion is due (in the model of SrS) to V_p and V_π as mentioned previously (also see Ref. 17). In addition, L_1 and L_3 are pushed down by the S p interaction with Sr d and s levels. The valence-band width found by Hasegawa and Yanase (and used in the present model) is a factor of 2 smaller than that suggested by the empirical rules of Pantelides.[18] Further refinement of the model awaits additional experimental and theoretical investigations.

III. RECURSION METHOD

In a random system, such as the pseudobinary alloy considered in this paper, the exact eigenstates ψ_m are generally too complicated to be determined and would probably not be useful even if they were known. Instead, other quantities such as the DOS have more physical meaning. In alloys, there are two types of partial or projected DOS that are particularly relevant to the characterization of the electronic structure: the local DOS (LDOS) and the $\vec{k}$-dependent spectral weight.

The LDOS is defined using an atomic basis set. Suppose that for each type of atom in the alloy, we have a set of $s,p,d,\ldots$ orbitals (as in the tight-binding model

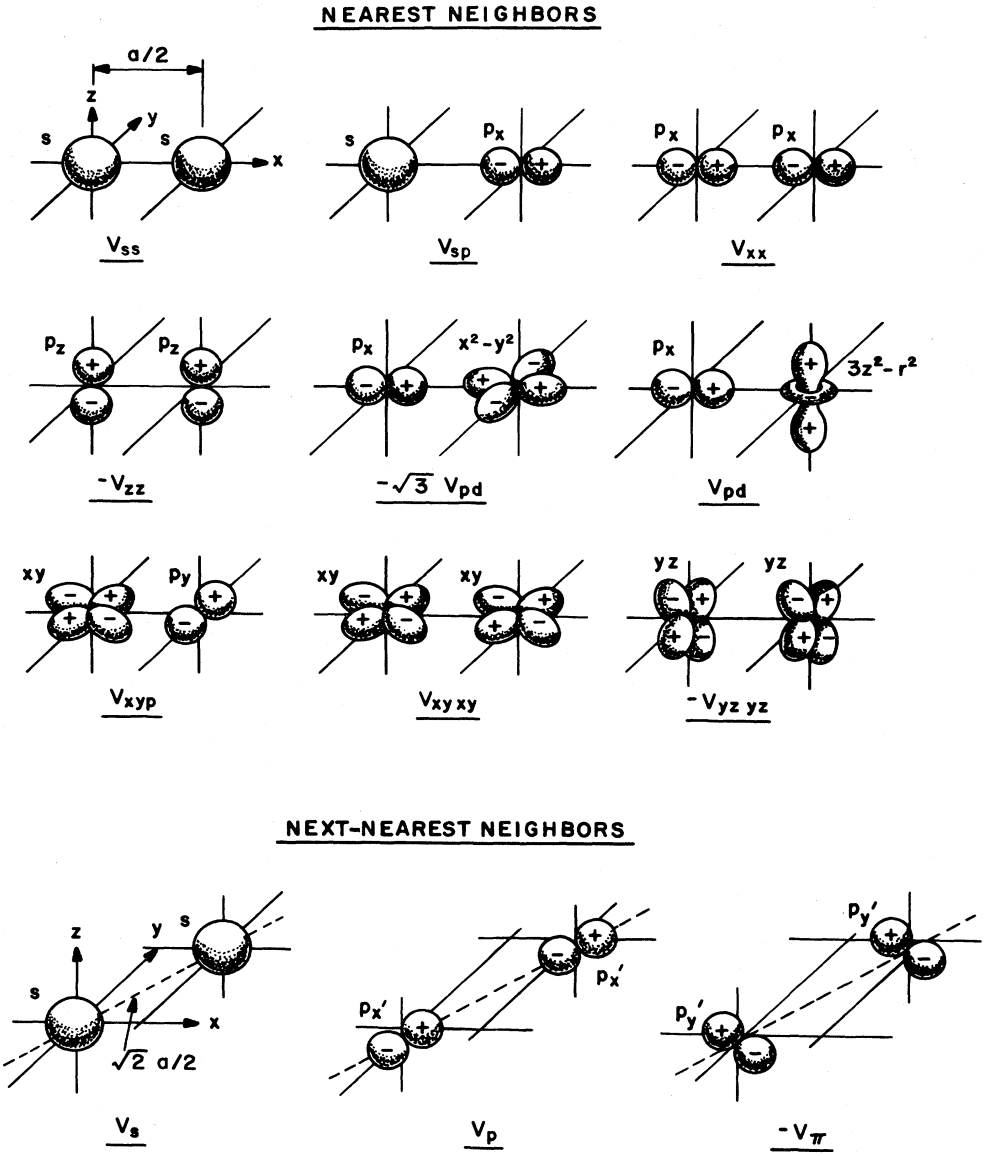

FIG. 2. Pictorial representation of the matrix elements which enter the tight-binding model discussed in the text. See Tables II and III for further definitions and notations. Orbitals $p_{x'}$ and $p_{y'}$ are parallel and perpendicular, respectively, to the [110] direction.

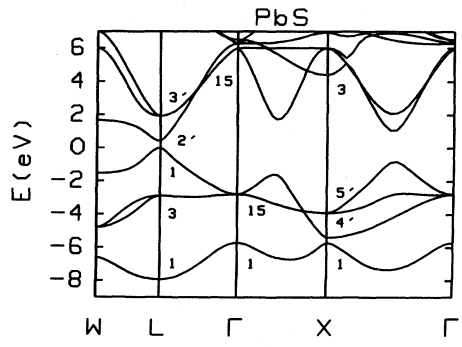

FIG. 3. Band structure of PbS based upon the tight-binding model described in the text.

described in Sec. II). Let us denote them by $\phi_n(\vec{r}-\vec{R})$, where $\vec{R}$ is the atomic position. We can expand any eigenstate of the alloy Hamiltonian in terms of the atomic basis according to

$$\psi_m(\vec{r})=\sum_{n,\,\vec{R}} C_{mn}(\vec{R})\phi_n(\vec{r}-\vec{R})\,. \tag{1}$$

The integrated LDOS is defined as

$$N_n(\vec{R};E)=\sum_{m,\,(E_m<E)} |\,C_{mn}(\vec{R})\,|^2\,. \tag{2}$$

This is a monotone function which increases from zero at low E to unity at high energy. The LDOS itself is the derivative with respect to E,

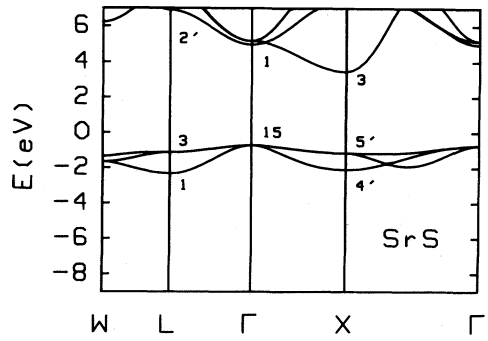

FIG. 4. Band structure of SrS based upon the tight-binding model described in the text.

$$n_n(\vec{R};E)=\frac{dN_n(\vec{R};E)}{dE} . \tag{3}$$

The LDOS represents the energy distribution among the eigenstates of the orbital n at the site $\vec{R}$. For alloys, it is often more sensible to look at the average over all sites. More precisely, averages over all cation or all anion sites will be computed. The total DOS is just the sum over all LDOS or partial DOS.

The second type of projected DOS is the $\vec{k}$-dependent spectral weight, $A(\vec{k},E)$. Although crystal symmetry is lacking in alloys, the remnants of band structure are present to some degree. For example, one could ask what happens to the band-edge states of PbS as Sr is added. To do this, let $\psi_{\vec{k}}$ be a Bloch function of a given symmetry at some position $\vec{k}$ in the Brillouin zone (e.g., L_1 or $L_{2'}$). Here,

$$\psi_{\vec{k}}=(N_0)^{-1/2}\sum_{\vec{R}} e^{i\vec{k}\cdot\vec{R}}\phi(\vec{r}-\vec{R}) , \tag{4}$$

where the sum is over all N_0 cation or anion sites and ϕ is a linear combination of atomic functions appropriate to the given symmetry of $\psi_{\vec{k}}$. Note that in the alloy, if we consider a state that involves the cation sites which are randomly Pb or Sr, $\phi(\vec{r}-\vec{R})$ is made up of Pb functions on Pb sites and Sr functions on Sr sites. Now for the pure crystal, as $\psi_{\vec{k}}$ is defined, it may not be the eigenstate of the Hamiltonian, but it will be of the same symmetry and be a component of the eigenstate. The integrated spectral weight is defined similar to Eq. (2) but with a weighting factor $|\langle\psi_{\vec{k}}|\psi_m\rangle|^2$. Hence,

$$A(\vec{k},E)=\sum_m |\langle\psi_{\vec{k}}|\psi_m\rangle|^2\delta(E-E_m) , \tag{5}$$

which is analogous to Eq. (3).

The LDOS and the spectral weight can be determined using the Haydock recursion method.[7,20] With this method, one can calculate an upper and a lower bound to an integrated DOS, such as $N_n(\vec{R};E)$. An estimate, typically the average of the bounds, is made for the integrated DOS and then the DOS itself is found by numerically differentiating.

A large cluster ($\sim$1000 atoms) is generated, the cations being chosen as Pb or Sr at random according to the concentration. The recursion method is then applied to this large cluster. (If short-range order were present and the cluster generated appropriately, the method could be applied equally well—a feature not exploited in the present work.)

Having chosen some state u_0 upon which we want to project the eigenstates of the Hamiltonian H, we set up a recursion. The start state u_0 would be $\phi_n(\vec{r}-\vec{R})$ if we wish to calculate $N_n(\vec{R};E)$. The first recursion equation is

$$Hu_0=a_0u_0+b_1u_1 . \tag{6}$$

Here a_0 is the average of H with respect to u_0, $(u_0|H|u_0)$, and b_1u_1 is the remainder of Hu_0 after its projection on u_0 is removed. All states u_n are assumed normalized, so b_1 is the length of $(H-a_0)u_0$. By convention, all quantities are taken to be real and the b_n positive. The second equation in the recursion is

$$Hu_1=a_1u_1+b_1u_0+b_2u_2 . \tag{7}$$

Subsequent equations are of the same form as (7), that is, a three-term recursion:

$$Hu_n=a_nu_n+b_nu_{n-1}+b_{n+1}u_{n+1} . \tag{8}$$

The states u_n are orthonormal and if H is transformed into this basis, it has tridiagonal form. Namely,

$$(u_n|H|u_n)=a_n$$

and

$$(u_n|H|u_{n+1})=(u_{n+1}|H|u_n)=b_{n+1} .$$

Formally, the DOS

$$n_0(E)=\sum_m (u_0|\psi_m)^2\delta(E-E_m)$$

is the imaginary part (divided by $-\pi$) of a Green's function,

$$G(E)=\cfrac{1}{E-a_0-\cfrac{b_1^2}{E-a_1-\cfrac{b_2^2}{E-a_2-\cdots}}} , \tag{9}$$

where E has an infinitesimal positive imaginary part. $G(E)$ is merely the 0,0 element of $1/(E-H)$, and it is straightforward to show that it can be expressed in the continued-fraction form (9). The advantage of the recursion method is that the continued fraction converges rapidly. Typically, the number of recursions L may only be 10–20 for a Hamiltonian which is of order N equal to a few hundred or more. Of course, when $L+1=N$, the method is exact. For smaller L, resolution in energy is lost; band edges are smeared out. Also, the upper and lower bounds on the integrated DOS differ and if this becomes severe enough, the average when differentiated will falsely give two peaks where a single peak should be, one from each bound.

As a final topic in this section, let us examine the LDOS averaged over sites in the alloy. One could

separately calculate $n_n(\vec{R};E)$ for each site and then add. However, it is computationally much faster to prepare a start state u_0 which is a (properly normalized) sum of random $(\pm)\,\phi_n(\vec{r}-\vec{R})$, the sum being over all cation or anion states.[20] Since $G(E)$ is $(u_0\,|\,(E-H)^{-1}\,|\,u_0)$, this start state will give a sum of site-diagonal terms $(\phi_n(\vec{R})\,|\,(E-H)^{-1}\,|\,\phi_n(\vec{R}))$ plus off-diagonal terms of the same form, but different $\vec{R}$ vectors multiplied by a random sign. If the sample is infinite, the off-diagonal terms cancel out. For a finite sample, an ensemble of start states must, in principle, be constructed to obtain cancellation. In practice, for a large system only a few u_0 are required for convergence. That is, perhaps five or so u_0 states with randomly generated signs are constructed and the resultant LDOS are added.

Similar techniques have used for the vibrational and the electronic spectra of amorphous solids.[6] These results suggest that the application of the method to the electronic structure of alloy should also be fruitful. The convergence with the number of recursions and the effects of cluster size have been discussed by other authors.[7,5]

IV. NUMERICAL RESULTS

The calculations reported in this section are based upon the application of the tight-binding model (discussed in Sec. II) and the recursion method (Sec. III) to large clusters of atoms. The crystal structure of the alloy is rocksalt so the position of any atom in the cluster is given by $\vec{R}=\frac{1}{2}a\,(n,m,l)$. The sulfur anions are on one fcc sublattice and the cations (Pb and Sr) are on the other. Each atom is described by the atomic orbital energies given in Table I and its interaction with other atoms by the matrix elements given Tables I and III and Fig. 2. No Sr-Pb interaction has been included, although it would be straightforward to do so.

The DOS for the pure materials are shown in Figs. 5–7. Throughout the paper, the units for any DOS displayed are states/eV spin (unit cell). The results from two different methods of calculating the total DOS for PbS are given in Fig. 5. The solid curve is from summing the LDOS for all orbitals in a unit cell near the center of a $12\times10\times8$ cluster. Thirty-one recursions were used. The dashed curve was calculated by averaging the DOS from five u_0, each a linear combination of random $(\pm)\phi$, where ϕ is the sum of all orbitals on a site (see Sec. III). Periodic boundary conditions were used for the latter case. The number of recursions was 48 as it was for all calculations

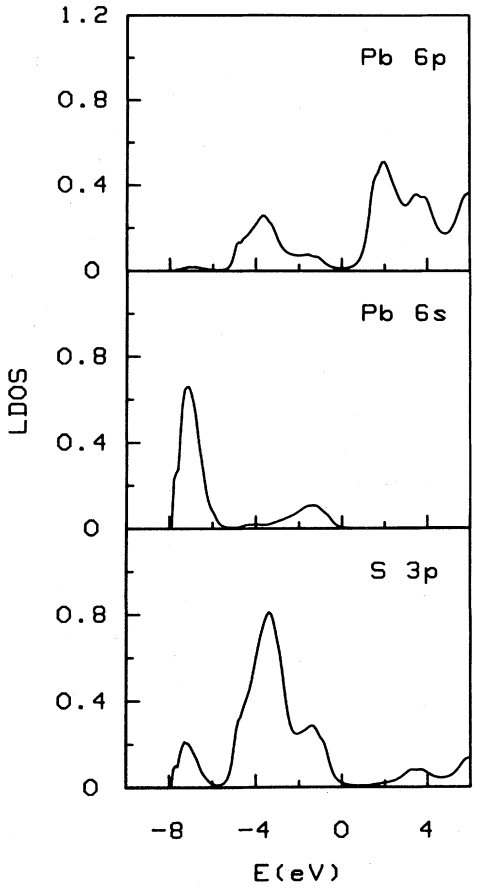

FIG. 6. LDOS for the three principal constituents of the density of states (solid curve) in Fig. 5.

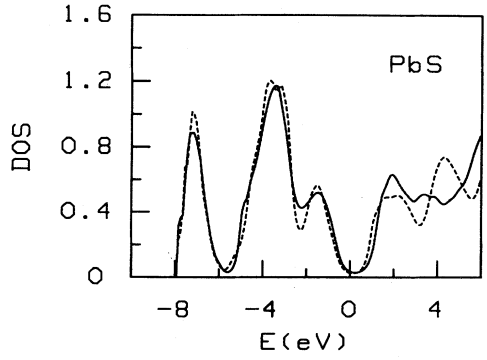

FIG. 5. DOS for PbS. Solid curve is from summing the local density of states in a unit cell at the center of a $12\times10\times8$ cluster (31 recursions). Dashed curve from a $12\times10\times8$ cluster with periodic boundary conditions (48 recursions). Start state u_0 involved random sign $(\pm)$ on each site.

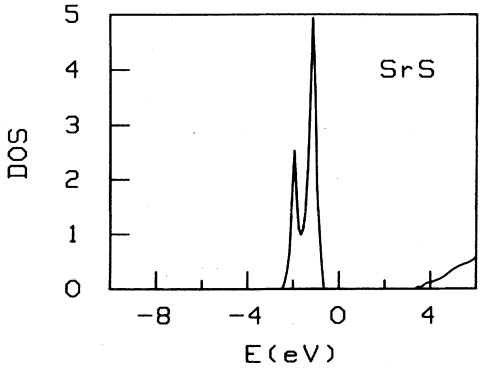

FIG. 7. DOS of SrS calculated in the same manner as the dashed curve in Fig. 5, but with a $12\times12\times8$ cluster (48 recursions).

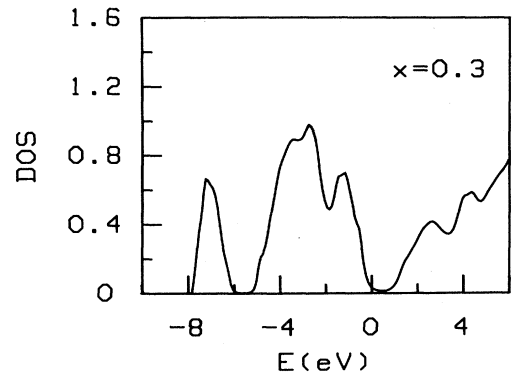

FIG. 8. DOS for $Pb_{0.7}Sr_{0.3}S$ calculated as in Fig. 7.

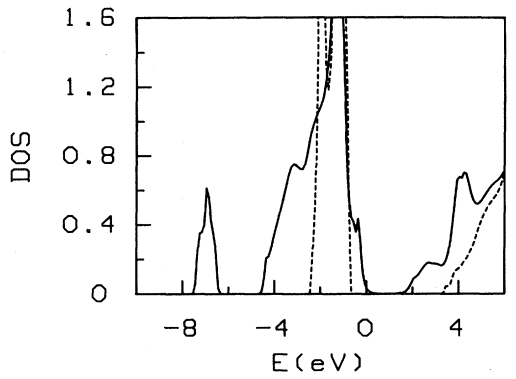

FIG. 10. DOS for $Pb_{0.3}Sr_{0.7}S$ (solid curve) and pure SrS (dashed curve). Calculated as in Fig. 7.

reported, unless noted otherwise. Other than the lower resolution for the sum of LDOS (due to fewer recursions), there is good agreement between the two methods in the region of the valence bands. The conduction band is more sensitive to the boundaries (structure dependent on cluster size and shape) and consequently the results from the two methods differ somewhat. The limited resolution of the calculation obscures the small gap (0.4 eV) in the DOS. In general, however, the results are fairly close to those of Kohn *et al.*[12]

Individual LDOS for the three largest components are shown in Fig. 6 (calculated by the same method as the solid line in Fig. 5). The S 3*p* LDOS is mostly in the valence band and the Pb 6*p* LDOS is mostly in the conduction band, but considerable mixing due to V_{xx} is observed. The Pb 6*s* intensity in the valence band is due to V_{sp}.

The DOS for pure SrS is shown in Fig. 7. It was calculated in the same manner as the dashed curve in Fig. 5. The cluster size was $12\times12\times8$ and the number of recursions was 48. Periodic boundary conditions were imposed. Note the change in vertical scale in Fig. 7 relative to Fig. 5. The valence band has a much higher peak DOS and is narrower than for PbS. The valence electrons are mainly S 3*p*. The conduction band which starts at 3.4 eV is broader and less dense than the valence band.

Alloy DOS's are displayed in Figs. 8—11. They were calculated in the same way as Fig. 7 and the dashed line in Fig. 5. The figures are labeled by the nominal concentrations of Sr; the actual values are 0.306, 0.510, 0.703, and 0.944. By calculating the LDOS, such as in Fig. 6, for the alloys, the atomic character of the DOS can be determined. For example, it has been established that Pb *s* states are the predominant component in the region -8 to -6 eV as expected. The Pb *s* intensity decreases and becomes narrower as x increases. The valence band narrows also, although the total intensity remains constant. The energy gap between the valence and conduction bands opens up, principally by the conduction band moving to higher energy. For x near 1, Pb impurity levels appear (*s*-like states near 0 and *p*-like near 3 eV; see Ref. 17) which are barely visible on the scale of Fig. 11.

The $\vec{k}$-dependent spectral weight $A(\vec{k},E)$ is shown for several points in the Brillouin zone and various concentrations in Figs. 12—15. The first is for a cluster of $12\times8\times8$ atoms and 41 recursions whereas the rest are for $12\times12\times8$ and 48 recursions. Periodic boundary conditions are essential for calculating the spectral weight, otherwise there is too much surface scattering. Only a limited number of $\vec{k}$ vectors are consistent with the cluster size and periodic boundary conditions, namely those for which $k_x=(4\pi/a)(n_x/N_x)$, where n_x is an integer and $N_xa/2$ is the x dimension of the cluster, etc. To restrict the calculation to real quantities, the exponential in Eq. (4) is re-

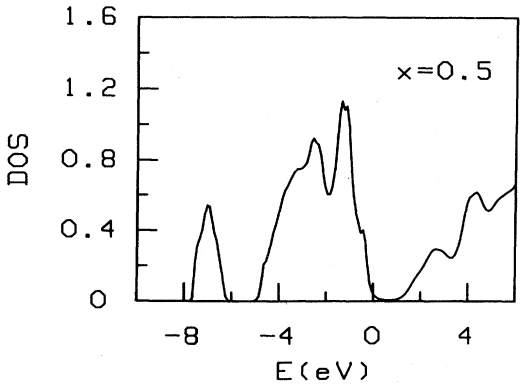

FIG. 9. DOS for $Pb_{0.5}Sr_{0.5}S$ calculated as in Fig. 7.

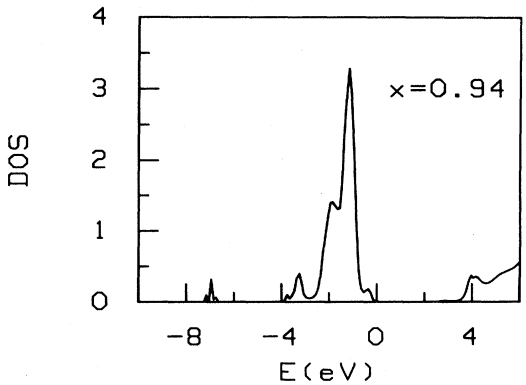

FIG. 11. DOS for $Pb_{0.06}Sr_{0.94}S$ calculated as in Fig. 7.

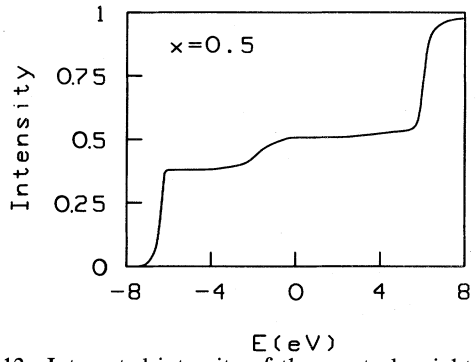

FIG. 12. Integrated intensity of the spectral weight function for Γ_1 vs energy for $Pb_{0.5}Sr_{0.5}S$. Start state u_0 involved s orbital on each cation site ($12\times8\times8$ cluster, 41 recursions).

placed by $\cos(\vec{k}\cdot\vec{R})$.

The integrated spectral weight for $\Gamma_1(\vec{k}=0)$ is plotted in Fig. 12. The ϕ in Eq. (4) is the s orbital on each cation site. The Γ_1 state, which is at -5.7 eV in PbS and 5.0 eV in SrS, is split into two parts in the alloy. Approximately half of the intensity is below the gap and half above. The peaks in $A(\vec{k},E)$ (derivative of Fig. 12) occur at -6.3 eV and 6.0 eV. These differ from the pure crystal because there is less dispersion, a result of fewer like neighbors. Since symmetry is broken by disorder in the alloy, the V_{sp} interaction produces some intensity in the valence band, even though none exists at Γ in either pure crystal. The derivations from virtual-crystal behavior are considerably larger than those for s states in $Hg_{1-x}Cd_xTe$.[9]

Although the original data of Holloway and Jesion[1] suggested that the direct gap at X in SrS decreases as Pb is added, Fig. 13 indicates otherwise. The dashed curve is the spectral weight (divided by 3) for the X_3 state ($\phi=yx$ on the cations) which peaks at 3.66 eV for $x=0.7$ compared to 3.44 eV for $x=1$. The $X_{5'}$ state ($\phi=p_y$ on the anions) shifts insignificantly, $E=-1.19$ eV relative to -1.16 eV for pure SrS. Comparing to Fig. 10, we see that the reduction of the apparent gap in the DOS (as well as

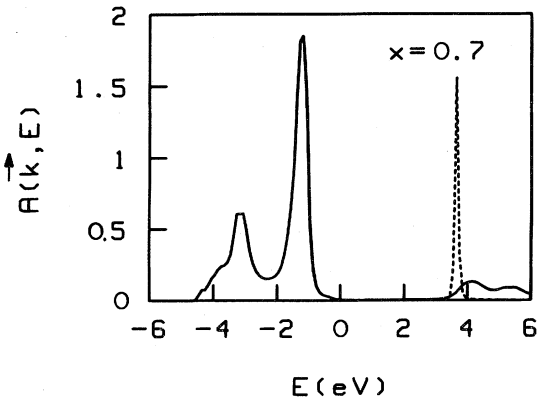

FIG. 13. Spectral weights for X_3 (divided by 3, dashed curve) and $X_{5'}$ (solid curve) for $Pb_{0.3}Sr_{0.7}S$. Start state u_0 involved yz orbital on each cation site for X_3 and p_y on each anion site for $X_{5'}$ ($12\times12\times8$ cluster, 48 recursions).

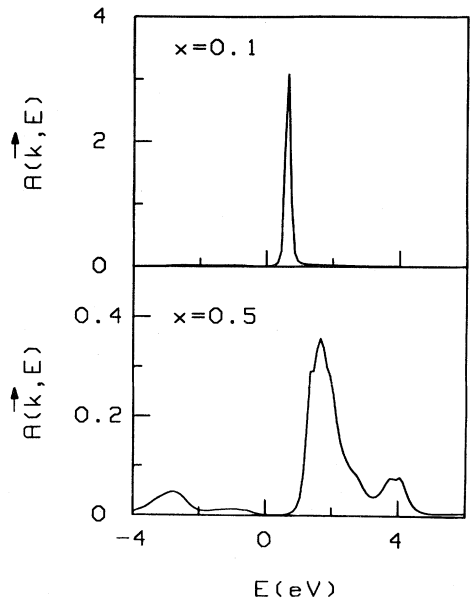

FIG. 14. Spectral weights for $L_{2'}$. Start state u_0 involved $p_x+p_y+p_z$ on each cation site ($12\times12\times8$ cluster, 48 recursions).

the absorption edge) is not due to the changes in the direct gap at X in the alloy, but rather due to the formation of the Pb impurity band. It is not surprising that the gap at X increases with the addition of Pb to SrS, since the $X_{5'}$-X_3 separation in PbS is about 4 eV larger than in SrS.

The nature of the states that exist in the region from the conduction-band edge down to about 2 eV is not entirely clear. It can be shown, however, that Pb $6p$ orbitals are the dominant constituent, rather than cation s or d. The

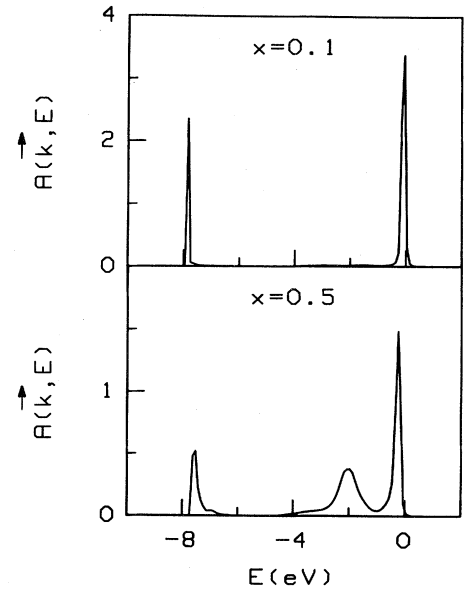

FIG. 15. Spectral weights for L_1. Start state u_0 involved $p_x+p_y+p_z$ on each anion site. Mixing due to V_{sp} causes peak near -8 eV. It also exists in pure PbS ($12\times12\times8$ cluster, 48 recursions).

states may have a mobility edge and may show an Anderson transition.[21] In contrast to the impurity band in a heavily doped semiconductor (e.g., Si:P), the Pb impurity band is unusual in two respects. First, it exists on an electron-volt scale rather than on a milli-electron-volt scale. Second, it does not (to first order) contain any carriers. That is, increasing the Pb concentration in SrS does not add electrons to the impurity band.

In Figs. 14 and 15, the spectral weights for states at L are shown for $x=0.099$ and 0.510. Since the gap in PbS is due to the direct transition from L_1 to $L_{2'}$, the behavior of these states in the alloy is examined. The ϕ in Eq. (4) is $(p_x+p_y+p_z)/(3)^{1/2}$ on the cation (anion) sites for $L_{2'}$ (L_1) The $L_{2'}$ peak broadens and shifts to higher energies as x is increased. The L_1 peak shifts and broadens a little and a secondary peak develops near -2 eV (compare Fig. 13) as x is increased. The secondary peak is the SrS-like L_1 peak which occurs at -2.3 eV in pure SrS. The higher-energy peak goes over into the Pb s—like impurity state at -0.34 as $x\rightarrow 1$. (In Ref. 17, the model used did not contain d states and the impurity was at -0.42 eV). The $L_{2'}$ state is perturbed more by alloying than the L_1 state because the wave function for the latter is concentrated on the S sites, whereas the $L_{2'}$ state is on the cation sites. The peak near -8 eV is due to the coupling to the L_1 state derived from Pb 6s orbitals and, of course, exists in pure PbS as well. The $L_{2'}$ intensity below the gap in Fig. 14 (also $X_{5'}$ intensity above the gap in Fig. 13) is caused by the effects of disorder and the p-p interaction between Pb and S. The sharp peaks in Figs. 14 and 15 indicate well-defined quasiparticles at the band edges. The peak energies are plotted in Fig. 16. For $x=0.5$, the uncertainty in $L_{2'}$ is ~ 0.2 eV. The uncertainty in the L_1 energy is considerably less, only 0.04 eV.

For $x<0.5$, it is reasonable to compare the observed energy gap (optical absorption edge) to the energy separation between the peak energies for L_1 and $L_{2'}$. The calculated separation agrees reasonably well with the experimental results of Holloway and Jesion (see Fig. 17). There is, however, a problem in rigorously determining the gap in an alloy where substantial broadening and possibly tailing into the gap exists.

Since the Sr cation differs appreciably from Pb, the Sr ions act as dilution sites in this region of concentration.

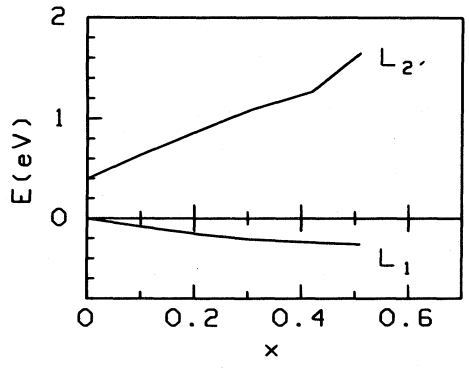

FIG. 16. Energies of peak in spectral weight vs concentration. The $L_{2'}$ energy has uncertainty of ± 0.2 eV near $x=0.5$.

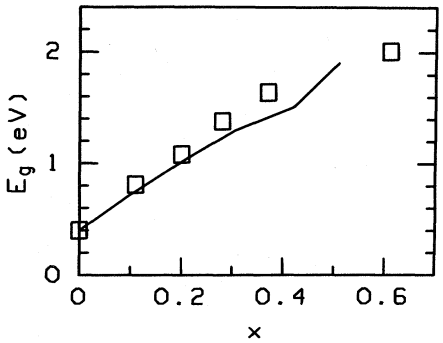

FIG. 17. Measured optical gap (absorption edge, Ref. 1) (squares) vs concentration compared to calculated $L_{2'}$-L_1 separation (solid line).

The energy gap would be approximately the same if the Sr ions in the alloy were replaced by equivalently charged vacancies. Experimentally, it is found that at a given x, $Pb_{1-x}Ca_xS$ has about the same gap as $Pb_{1-x}Sr_xS$.[1] This implies that the virtual-crystal approximation is substantial in error, in spite of the fact that well-defined quasiparticle states exist at L for small x.

The CPA cannot be applied easily to this alloy because of the mixing between valence and conduction bands. In this case, the CPA will involve coupled integral equations. The solution, without further approximation, will be more difficult than previous applications where this problem did not arise.[8] In Ref. 10, coupled integral equations were solved for $Hg_{1-x}Cd_xTe$. Only diagonal disorder was included since the nearest-neighbor Hg-Te and Cd-Te matrix elements are nearly the same. For the present problem, the off-diagonal matrix elements for PbS and SrS differ substantially and the recursion method may be more suitable than CPA for this reason.

V. CONCLUSIONS

Two main conclusions can be drawn from the work reported in this paper. First, a good understanding of the electronic structure of $Pb_{1-x}Sr_xS$ has been obtained. A tight-binding model has been found that describes fairly accurately the behavior of the valence and tightly bound states as well as the lower conduction states. As Sr is added to PbS, the direct gap at L increases as demonstrated by calculating the spectral weight $A(\vec{k},E)$. Agreement with experiment is quite favorable. At the other end of the concentration range, the gap at X (where the direct gap in SrS is supposed to be) actually increases as Pb is added to SrS. Owing to states consisting mostly of Pb 6p orbitals, the energy gap is the DOS, on the other hand, decreases (as observed empirically)—a unique situation in semiconductor alloys.

Cation s intensity splits into two parts in the alloy; one part below the valence band (due to Pb) and the other above the gap (due to Sr). This is decidedly unlike the virtual-crystal approximation where the s band would move through the gap as x increases. (Numerous other deviations have been noted, also.) However, even in this strongly scattering alloy (Pb and Sr differ substantially),

well-defined quasiparticle states have been found in certain regions of energy and $\vec{k}$ space.

The second aspect of this work has been to demonstrate the usefulness of the recursion method for alloy problems, particularly for real materials with multiple bands. A number of advantages of the method over the CPA have been listed in the Introduction and commented upon in the text. The limitations of the recursion method are not so fundamental as those of the CPA. Increasing the cluster size and the number of recursions brings the results closer to the exact results. I expect that the application of this method to other materials and related problems will be forthcoming.

ACKNOWLEDGMENTS

The author would like to thank Dr. H. Holloway and Dr. M. A. Tamor for numerous discussions and ideas regarding this work, L. Elie for help in preparing the figures, E. Ho and Professor J. D. Dow for a preliminary version of the tight-binding band-structure calulation and a number of helpful suggestions, Dr. E. P. O'Reilly for a copy of the Cambridge Recursion Library (written by C. M. M. Nex) and assistance in using it, Professor R. Haydock for a useful conversation, and K. Hass for pertinent remarks on the CPA.

APPENDIX

For the tight-binding model discussed in Sec. II and defined in Tables I to III, the band energies at symmetry points in the Brillouin zone are given in this appendix. At Γ and X, all eigenvalues can be expressed in pairs with the canonical form

$$E=(E_A+E_C)/2\pm[(E_A-E_C)^2+4V^2]^{1/2}/2 .$$

Both E_A and E_C are of the form of an anion or cation orbital energy (Table I) plus a dispersion contribution due to next nearest neighbors (Table III). The coupling V is from nearest-neighbor interactions (Table II). For example, the Γ_1 energy involves $E_C=E_s^{(C)}+12V_s^{(C)}$ and $V=6V_{ss}$. $V_s^{(C)}$ denotes the value for the cation; in the analogous expression for the anion, it would be the anion value (if different from zero). In tabular form, the entries in the canonical form for all eigenvalues are as follows.

State	Orbital	Dispersion	V
Γ_1	s	$12V_s$	$6V_{ss}$
Γ_{15}	p	$4(V_p-2V_\pi)$	$2(V_{xx}-2V_{zz})$
Γ_{12}	e_g		0
$\Gamma_{25'}$	t_{2g}		$2(2V_{xyxy}-V_{yzyz})$
X_1	s	$-4V_s$	$2V_{ss}$
$X_{4'}$	p	$-4V_p$	$2(V_{xx}+2V_{zz})$
$X_{5'}$	p	$4V_\pi$	$2V_{xx}$
$X_{1,2}$	e_g		0
X_3	t_{2g}		$2(2V_{xyxy}+V_{yzyz})$
X_5	t_{2g}		$2V_{yzyz}$

The eigenenergies at L can be found from a 3×3 matrix of the form

$$\begin{bmatrix} E_1 & V_{12} & V_{13} \\ V_{12} & E_2 & 0 \\ V_{13} & 0 & E_3 \end{bmatrix} .$$

For L_1,

$$E_1=E_p^{(A)}-4[V_p^{(A)}+V_\pi^{(A)}],\quad E_2=E_s^{(C)},\quad E_3=E_{t_{2g}}^{(C)} ,$$

$$V_{12}=2(3)^{1/2}V_{sp},\quad V_{13}=4V_{xyp} .$$

The roles of anion and cation are reversed for $L_{2'}$,

$$E_1=E_p^{(C)}-4[V_p^{(C)}+V_\pi^{(C)}],\quad E_2=E_s^{(A)},\quad E_3=E_{t_{2g}}^{(A)} ,$$

$$V_{12}=2(3)^{1/2}V_{ps},\quad V_{13}=4V_{pxy} .$$

For L_3,

$$E_1=E_p^{(A)}+2[V_p^{(A)}+V_\pi^{(A)}],\quad E_2=E_{e_g}^{(C)},\quad E_3=E_{t_{2g}}^{(C)} ,$$

$$V_{12}=2(6)^{1/2}V_{dp},\quad V_{13}=2V_{xyp} .$$

Likewise, for $L_{3'}$,

$$E_1=E_p^{(C)}+2[V_p^{(C)}+V_\pi^{(C)}],\quad E_2=E_{e_g}^{(A)},\quad E_3=E_{t_{2g}}^{(A)} ,$$

$$V_{12}=2(6)^{1/2}V_{pd},\quad V_{13}=2V_{pxy} .$$

[1]H. Holloway and G. Jesion, Phys. Rev. B 26, 5617 (1982).
[2]F. Herman, R. L. Kortum, I. B. Ortenburger, and J. P. Van Dyke, Jr., J. Phys. (Paris) Colloq. 29, C4-62 (1968).
[3]A. Hasegawa and A. Yanase, J. Phys. C 13, 1995 (1980).
[4]H. Ehrenreich and L. M. Schwartz, in *Solid State Physics,* edited by H. Ehrenreich, F. Seitz, and D. Turnbull (Academic, New York, 1976), Vol. 13, p. 149. In the virtual-crystal approximation, the potential in the alloy is replaced by the weighted average of the potentials of the components. A $\vec{k}$-dependent band structure can then be calculated because the lattice disorder has been removed. Energy levels tend to vary linearly with concentration between the extremes of the pure materials. In the strong scattering limit, this approximation fails to predict the splitting of a band into two seperate subbands resembling those of the pure components.
[5]P. J. Lin-Chung and T. L. Reinecke, Phys. Rev. B 27, 1101 (1983).
[6]Y. Ishii and T. Fujiwara, J. Phys. F 10, 2125 (1980); T. Fujiwara and Y. Tanabe, *ibid.* 9, 1085 (1979).
[7]R. Haydock, in *Solid State Physics,* edited by H. Ehrenreich, F. Seitz, and D. Turnbull (Academic, New York, 1980), Vol. 35, p. 215.
[8]A.-B. Chen and A. Sher, Phys. Rev. B 23, 5360 (1981).
[9]W. E. Spicer, J. A. Silberman, J. Morgen, I. Lindau, J. A. Wilson, A.-B. Chen, and A. Sher, Phys. Rev. Lett. 49, 948 (1982).
[10]K. C. Hass, H. Ehrenreich, and B. Velický, Phys. Rev. B 27, 1088 (1983).
[11]C. M. M. Nex, Cambridge Recursion Library (unpublished) (see *Solid State Physics,* Ref. 7, p. 78).

[12]S. E. Kohn, P. Y. Yu, Y. Petroff, Y. R. Shen, Y. Tsang, and M. L. Cohen, Phys. Rev. B 8, 1477 (1973).
[13]G. M. Stocks, W. M. Temmerman, and B. L. Gyorffy, Phys. Rev. Lett. 41, 339 (1978).
[14]H. Asonen, M. Lindroos, M. Pessa, R. Prasad, R. S. Rao, and A. Bansil, Phys. Rev. B 25, 7075 (1982).
[15]E. Ho and J. D. Dow (private communication).
[16]S. G. Louie, Phys. Rev. B 22, 1933 (1980).
[17]M. A. Tamor, L. C. Davis, and H. Holloway, Phys. Rev. B 28, 3320 (1983).
[18]S. T. Pantelides, Phys. Rev. B 11, 5082 (1975).
[19]G. A. Saum and E. Hensley, Phys. Rev. 113, 1019 (1959).
[20]M. J. Kelley, in *Solid State Physics,* Ref. 7, p. 312.
[21]E. N. Economou, S. Kirkpatrick, M. H. Cohen, and T. P. Eggarter, Phys. Rev. Lett. 25, 520 (1970).